Nonlinear Dyn (2014) 78:1193–1204
DOI 10.1007/s11071-014-1507-x

ORIGINAL PAPER

Chaos RBF dynamics surface control of brushless DC motor with time delay based on tangent barrier Lyapunov function

Shaohua Luo · Jiaxu Wang · Songli Wu · Ke Xiao

Received: 19 September 2013 / Accepted: 30 May 2014 / Published online: 24 June 2014

Abstract Non-dimensional mathematical model of brushless DC motor (BLDCM) system is presented here. BLDCM is known to produce chaotic phenomenon under certain conditions. This paper fuses dynamic surface control, radial basis function neural network, and adaptive technology to control the BLDCM, which overcomes the repetitive differentiation of the nonlinear terms of backstepping and the boundedness hypothesis of control gain predetermined. The tangent barrier Lyapunov function is also used for time-delay nonlinear system with parametric uncertainties. Simulation results under different conditions indicate that the proposed method works well to suppress chaos and effects of parameter variation.

Keywords TBLF · DSC · RBFNN · Chaos · BLDCM

1 Introduction

The dynamics on an attractor is said to be chaotic if there exists exponential sensitivity to initial conditions. For most cases involving differential equations, chaos usually occurs together with geometrical strangeness [1,2]. In a BLDCM system, the chaotic behavior leads to the intermittent oscillation of torque and speed, irregular current noise of the system, and unstable control performance. Therefore, it intensively influences the stability of the system and safety as well [3]. The advantage of BLDCM is the elimination of the physical contact between the brushes and the commutators. Then, BLDCM is widely applied in direct-drive applications such as robotics [4] and aerospace [5].

For ameliorating the performance of the BLDCM system, a large amount of literatures and control methods have been attempted to apply in the motor drivers. For example, to speed up the error convergence rate, nonsingular fast terminal sliding-mode control (SMC) [6], which can reach finite-time stability, is applied. In Ref. [7], a high-order SMC method via backstepping is presented to attain finite-time tracking control regardless of mismatched disturbance. The Ott, Grebogi, and Yorke (OGY) method is a fundamental technology for controlling chaos [8,9]; unfortunately, choosing an adjustable parameter usually becomes very difficult. The neural fuzzy control (NFC) approaches can also achieve self-learning; however, it is difficult for online learning real-time control [10,11]. Chaos anti-control of three time scale brushless DC motors and chaos synchronization of different order systems are studied [12]. Anti-control of chaos of single time scale brushless DC motors and chaos synchronization of different order systems are proposed further [13].

S. Luo (✉) · J. Wang · S. Wu · K. Xiao
State Key Laboratory of Mechanical Transmission, Chongqing University, Chongqing 400044, China
e-mail: hua66com@163.com

S. Luo · S. Wu
College of Mechanical Engineering, Hunan University of Arts and Science, Hunan 415000, China

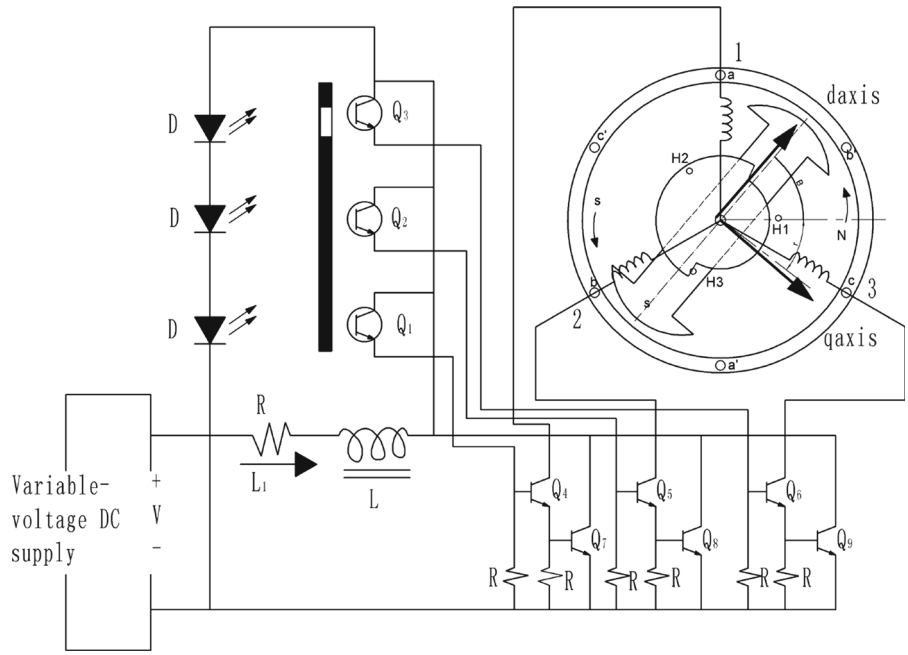

Fig. 1 The brushless DC motor system and its commutation

However, neither of them considers the time delay, output constraint, and unknown parameters.

Recently, a barrier Lyapunov function (BLF) which is proposed for constraint handling in Brunovaky-type system and nonlinear systems in strict feedback form are introduced for the special property of approaching infinity whenever its arguments approach some limits [14,15]. In addition, backstepping design method is an effective tool, which is often applied in nonlinear systems control with non-matching conditions, as well as systems with uncertain functions [16,17]. However, it suffers from repetitive differentiations. To solve this problem, the DSC is used to successfully overcome the shortage of traditional backstepping, and its first-order low-pass filter is used to gain the derivative information of the virtual control at the design procedure [18,19]. Control of chaos using the time-delay feedback control technology though is introduced to the real applications [20]. But it suffers from some problems as the control objective must be the equilibrium. Then, an adaptive DSC method is introduced to solve it for a class of uncertain time-delay nonlinear system with state constraint [21]. Using the high-gain observer, an adaptive fuzzy backstepping output feedback control approach is developed for a class of multiple-input and multiple-output (MIMO) nonlinear systems with time delays and immeasurable states [22]. For a class of MIMO stochastic nonlinear systems with immeasurable states, an adaptive fuzzy backstepping output feedback DSC approach is presented [23].

To the best of our knowledge, the combination among adaptive DSC, TBLF, and RBFNN has been seldom applied in the control of chaos for the BLDCM system yet. Further contribution includes the design of adaptive RBFNN DSC controller to handle uncertain time delays and parametric uncertainties. The proposed controller owns the suppression of the chaotic behavior, in addition to driving the system to the pre-defined trajectory with high precision and short response time. Meanwhile, the complexity of the designed controller is reduced, and the design procedure is much simpler than that of traditional backstepping. Simulation results show that control scheme is able to reduce chaos and effects of parameter variation. Similarly, the results are presented to show the effectiveness and robustness to control the BLDCM.

2 System descriptions and mathematical preliminaries

2.1 System descriptions

The brushless DC motor system considered here is illustrated in Fig. 1. It is an electromechanical system, and its equations of electrical and mechanical dynamics can be written in the following forms [12,24]:

Table 1 The denotation of the BLDCM parameters

Parameter	Denotation
i_d	The direct-axis currents (A)
ω	The rotor angular speed (rad/s)
v_d	The direct-axis voltage (V)
J	The moment of inertia (kgm^2)
L_d	The direct-axis fictitious inductance (H)
$k_t = \sqrt{3/2}k_e$	The permanent magnet flux (Wb)
k_e	The permanent magnet flux constant
i_q	The quadrature-axis currents (A)
n	Number of permanent pole pairs
v_q	The quadrature-axis voltage (V)
R	The winding resistance (Ω)
L_q	The quadrature-axis fictitious inductance (H)
b	The viscous damping coefficient (N/rad/s)
$\bar{T}_L$	The additional terms

$$\begin{cases} \frac{d\omega}{dt} = \frac{n}{J}\left[k_t i_q + \left(L_d - L_q\right) i_q i_d\right] - \frac{1}{J}\left(b\omega + \bar{T}_L\right) \\ \frac{di_q}{dt} = \frac{1}{L_q}\left[-Ri_q - n\omega\left(L_d i_d + k_t\right) + v_q\right] \\ \frac{di_d}{dt} = \frac{1}{L_d}\left[-Ri_d + nL_q\omega i_q + v_d\right] \end{cases} \tag{1}$$

The denotations of the BLDCM system parameters are shown in Table 1. In order to reduce the number of parameters, a transformation is carried out in the next section. Suppose the multiple time scales $\tau_1,\ \tau_2,\ \tau_3$ are defined as follows:

$$\begin{cases} \tau_1 = JR/k_t^2 \\ \tau_2 = L_q/R \\ \tau_3 = L_d/R \end{cases}, \tag{2}$$

where $\tau_1,\ \tau_2$, and τ_3 denote the mechanical time constant, the first electrical time constant, and the second electrical time constant, respectively.

Then, the new state space model for the BLDCM becomes

$$\begin{cases} \tau_1 \frac{dx_1}{dt} = \sigma x_2 + \rho x_2 x_3 - \eta x_1 - T_L \\ \tau_2 \frac{dx_2}{dt} = -x_2 - x_1 - x_1 x_3 + u_q \\ \tau_3 \frac{dx_3}{dt} = x_1 x_2 - x_3 + u_d \end{cases}, \tag{3}$$

where the non-dimensional variables are

$$x_1 = \frac{nL_q}{R\sqrt{\delta}}\omega, \quad x_2 = \frac{L_q}{k_t\sqrt{\delta}} i_q, \quad x_3 = \frac{L_q}{k_t\delta} i_d,$$

$$u_q = \frac{L_q}{k_t R\sqrt{\delta}} v_q, \quad u_d = \frac{L_q}{k_t R\delta} v_d, \quad \sigma = n^2,$$

$$\rho = (1-\delta)n^2, \quad \eta = \frac{Rb}{k_t^2}, \quad T_L = \frac{nL_q}{k_t^2\sqrt{\delta}}\bar{T}_L, \quad \delta = \frac{L_q}{L_d}.$$

It can be easily seen that the mathematical model of BLDCM owns high nonlinearity because of the coupling between the speed and the currents. In Eq. (3), T_L presents the normalized load torque; u_q and u_d denote the normalized quadrature-axis and direct-axis stator voltage, respectively; and $\sigma,\ \eta$, and ρ are unknown system parameters.

In order to show the computational results such as phase portrait, strange attractor, choose the parameters as $u_q = 4.017,\ u_d = -15.305,\ \tau_1 = 1,\ \tau_2 = 6.45,\ \tau_3 = 7.125,\ T_L = 2.678$, and select the true values of unknown parameters as $\sigma = 16,\ \rho = 1.516$ for chaos condition. The initial conditions of the drive systems are $x_1(0) = x_2(0) = x_3(0) = 0$. Figure 2 illustrates the phase portrait of various η. The motion is periodic in the situations of $\eta = 3.0,\ 2.36$. However, in the situations of $\eta = 2.1,\ 1.6$, the motion appears chaotic behavior, and $\eta = 2.34$ is a critical value. Figure 3 shows the strange attractor in BLDCM with parameter $\eta = 1.6$. Figure 4 shows the bifurcation diagram.

A time delay in the overall system can lead to voltage and current distortions due to the low-pass filter, hysteresis control inverter, microprocessor program computation time, and so on. Then, the mathematical model of BLDCM with uncertain nonlinear time delay is rewritten as follows:

$$\begin{cases} \dot{x}_1 = \frac{1}{\tau_1}\left[\sigma x_2 + \rho x_2 x_3 - \eta x_1 - T_L + \Delta f_1(x_1(t-\tau_1))\right] \\ \dot{x}_2 = \frac{1}{\tau_2}\left[-x_2 - x_1 - x_1 x_3 + u_q + \Delta f_2(\bar{x}_2(t-\tau_2))\right] \\ \dot{x}_3 = \frac{1}{\tau_1}\left[x_1 x_2 - x_3 + u_d + \Delta f_3(x_3(t-\tau_3))\right] \end{cases}, \tag{4}$$

where $\bar{x}_2(t) = [x_1(t), x_2(t)]^T$, $\Delta f_i(x_i(t-\tau_i)),\ i = 1, 2, 3$, denote the nonlinear time delay item, and $\tau_i,\ i = 1, 2, 3$, stand for the time delay constant.

For any given continuous signal y_r, the dynamics surfaces are defined as

$$\begin{cases} S_1(t) = x_1 - y_r \\ S_2(t) = x_2 - a_{2f} \\ S_3(t) = x_3 \end{cases}, \tag{5}$$

where a_{2f} is the filtered virtual controller.

Assumption 1 The nonlinear time delay items satisfy the following inequality:

$$\begin{cases} |\Delta f_1(x_1(t-\tau_1))| \le |S_1(t-\tau_1)|\, q_{11}(S_1(t-\tau_1)) \\ |\Delta f_2(\bar{x}_2(t-\tau_2))| \le |S_1(t-\tau_2)|\, q_{21}(S_1(t-\tau_2)) \\ \quad + |S_2(t-\tau_2)|\, q_{22}(\bar{S}_2(t-\tau_2)) \\ |\Delta f_3(x_3(t-\tau_3))| \le |S_3(t-\tau_3)|\, q_{31}(S_3(t-\tau_3)) \end{cases}, \tag{6}$$

where the nonlinear functions q_{11}, q_{21}, q_{22}, and q_{31} are known, $\bar{S}_2(t) = [x_1(t), x_2(t)]^T$.

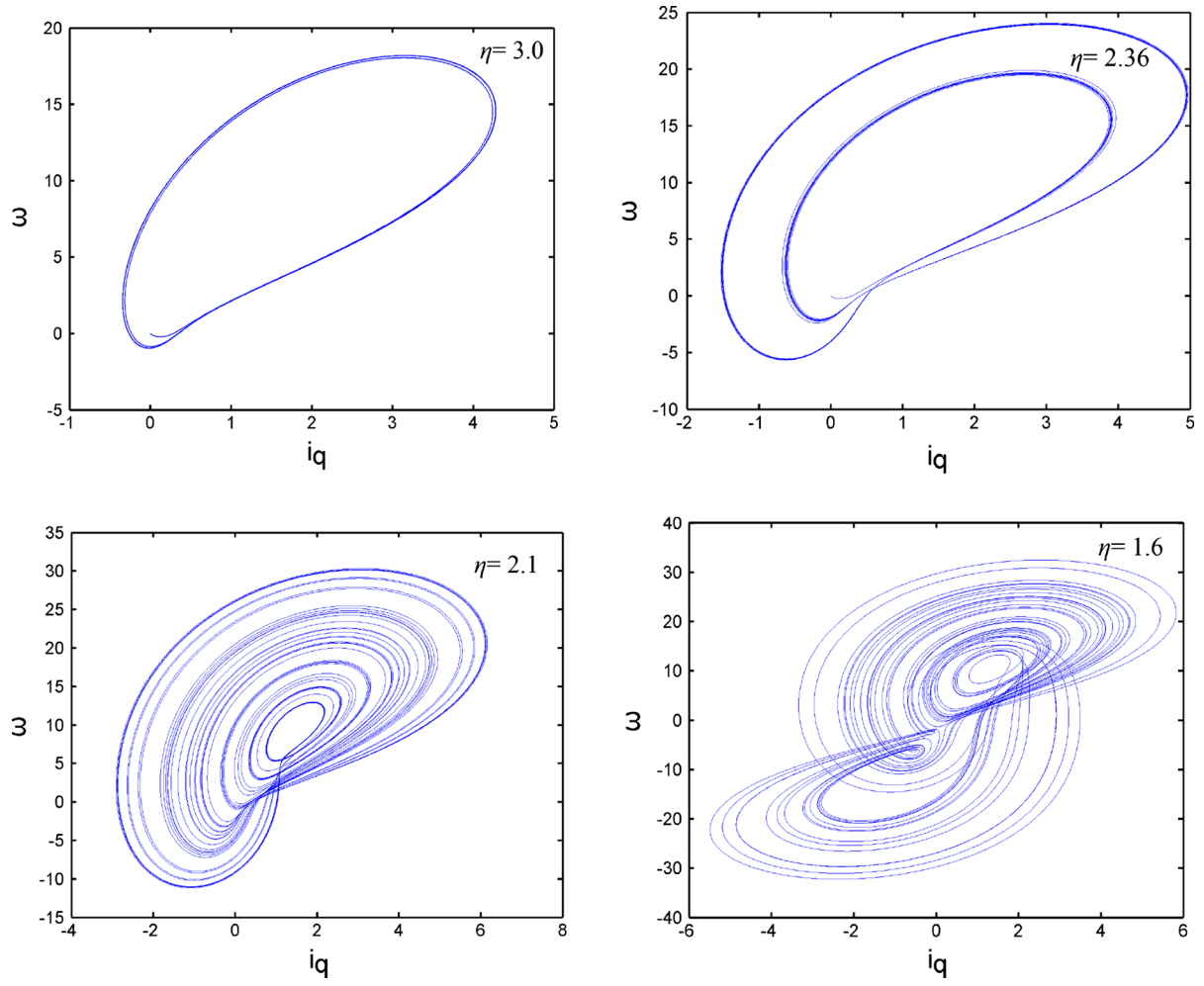

Fig. 2 Phase portrait with different η

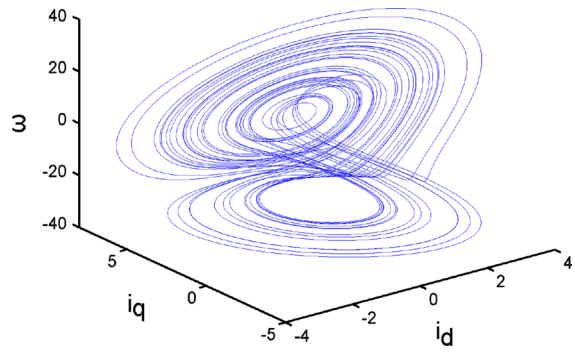

Fig. 3 Strange attractor with parameter $\eta = 1.6$

Assumption 2 The reference trajectory y_r is bounded by $-d \leq y_r \leq d$, $(a > d > 0)$, and the time derivatives $y_r^{(1)}$, $y_r^{(2)}$ are bounded.

The constraints are not violated in the whole dynamic process. That is, $x_1(t) \in (-a, a)$, $\forall t > 0$, where the constant $a > 0$.

2.2 Tangent barrier function

For the sake of ensuring that system state is bounded in a desired region, a tangent barrier function $y\tan(y)$ is employed in this paper, where $\tan(\cdot)$ stands for the tangent function. It is obvious that the tangent barrier function satisfies the characteristics listed as below:

$$+\infty > y\tan(y) \geq 0 \text{ for } y \in (-\pi/2, \pi/2). \quad (7)$$

According to the above descriptions, we can formalize the results for general forms of tangent barrier function in Lyapunov synthesis satisfying $y\tan(y) \to \infty$ as $y \to -\pi/2$ or $y \to \pi/2$.

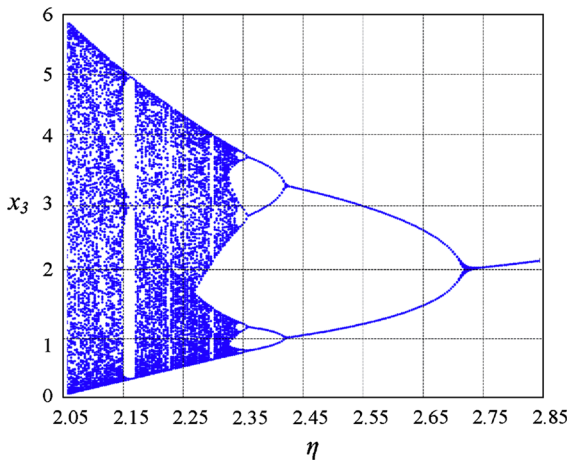

Fig. 4 Bifurcation diagram

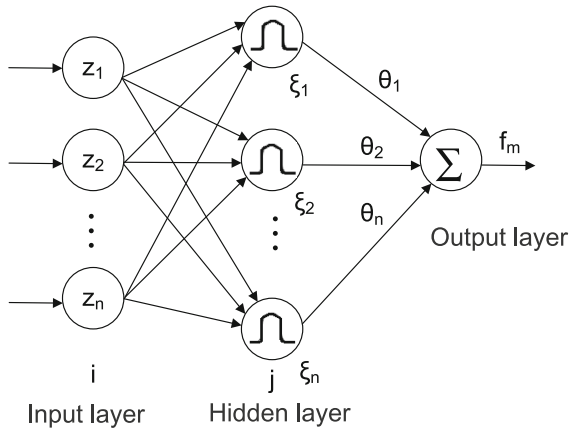

Fig. 5 The structure of the RBFNN

3 Design of chaos controller based on TBLF

3.1 RBFNN

For the continuous function $f(\theta, z)$and bounded closed set $\Omega \to R^n$, there is a RBFNN shown in Fig.5, which satisfies

$$f(\theta, z) = \theta^T \xi(z) + \varepsilon, \tag{8}$$

where $z \in \Omega \subset R^n$ is the input vector with n being the neural network input dimension, Ω denotes some compact set in R^n, $\theta = [\theta_1, \theta_2, \cdots, \theta_n]^T \in R^l$ is the weight vector, and $l > 1$ is the node number of neuron.ε is the estimation error, and $\xi(z) = [\xi_1(z), \xi_2(z), \cdots, \xi_n(z)]^T \in R^l$ is a basic function vector.

The Gaussian basis function is selected as

$$\xi_i(z) = \exp\left[-\frac{\|z - \mu_i\|^2}{2\sigma_i^2}\right], i = 1, 2, \cdots, l \tag{9}$$

where $\mu_i = [\mu_{i1}, \mu_{i2}, \cdots, \mu_{in}]^T$ is the center of basic function $\xi_i(z)$, σ_i is the width of $\xi_i(z)$, and $\|\cdot\|$ denotes the 2-norm of a vector.

Define the best weight vector as

$$\theta^* = \arg\min_{\theta \in R^n}\left\{\sup_{z \in \Omega}\left\|f(z) - \widehat{\theta}^T \xi(z)\right\|\right\}. \tag{10}$$

Assumption 3 There is a positive constant ε_M which satisfies $|\varepsilon_i| \le \varepsilon_M, i = 1, 2, 3$

3.2 Controller design

Theorem 1 *The special case of the Cauchy–Schwarz inequality in a Euclidean space is called Cauchy's inequality. It is one of the most important inequalities in all of mathematics [25]. It is usually written as*

$$\left(\sum r_i s_i\right)^2 \le \sum r_i^2 \sum s_i^2, \tag{11}$$

where all of $r_i, \quad s_i \in R$.

According to the above-mentioned dynamics system, the whole design process consists of three phases. Then, the process of the design is given in detail.

Step 1: Calculate the derivative of S_1

$$\dot{S}_1 = \frac{1}{\tau_1}\left[\sigma x_2 + f_1 + \Delta f_1(x_1(t - \tau_1))\right] - \dot{y}_r, \tag{12}$$

where $f_1 = \rho x_2 x_3 - \eta x_1 - T_L$.

Based on the above description, σ, η and ρ are unknown parameters of system. Then, it is not easy to construct the controller for traditional methods. To cope with this problem, adaptive technique is employed to deal with the unknown gain, and RBFNN is used to approximate the uncertain nonlinear function f_1. Therefore, for any given ε_1, there exists a RBFNN $\theta_1^T \xi_1$ such that

$$f_1 = \theta_1^T \xi_1 + \varepsilon_1, \tag{13}$$

where ε_1 is the approximation error and satisfies

$|\varepsilon_1| \le \varepsilon_M$.

Substituting Eq. (13) into Eq. (12), it is obtained

$$\dot{S}_1 = \frac{1}{\tau_1}\left[\sigma x_2 + \theta_1^T \xi_1 + \Delta f_1(x_1(t - \tau_1))\right] - \dot{y}_r. \tag{14}$$

Choose a TBLF candidate as

$$V_1 = \tau_1 S_1(t)\tan\left(\frac{\pi}{2\beta}S_1(t)\right) + \sum_{i=1}^{2}\int_{t-\tau_i}^{t} S_1^2(t)\,q_{i1}^2(S_1(t))\mathrm{d}\tau + \frac{1}{2\gamma_1}\tilde{\theta}_1^T\tilde{\theta}_1 + \frac{1}{2\Gamma_1}\tilde{\sigma}^2, \tag{15}$$

where the design parameter $\beta = a - d > 0 (a > d)$ denotes the constraint on $S_1(t)$. That is, $S_1(t) \in (-\beta, \beta)$.

Then, the time derivative of V_1 is calculated by

$$\begin{aligned}\dot{V}_1 &= \tau_1\dot{S}_1(t)\begin{bmatrix}\tan\left(\frac{\pi}{2\beta}S_1(t)\right) + \frac{\pi}{2\beta}S_1(t)\\ \sec^2\left(\frac{\pi}{2\beta}S_1(t)\right)\end{bmatrix}\\ &+\sum_{i=1}^{2} S_1^2(t)\,q_{i1}^2(S_1(t)) + \frac{1}{\gamma_1}\tilde{\theta}_1^T\dot{\widehat{\theta}}_1 + \frac{1}{\Gamma_1}\tilde{\sigma}\dot{\widehat{\sigma}}\\ &-\sum_{i=1}^{2} S_1^2(t-\tau_i)\,q_{i1}^2(S_1(t-\tau_i))\\ &=\left[\sigma(S_2 + y_2 + \alpha_2) + \theta_1^T\xi_1 - \tau_1\dot{y}_r\right]M\\ &+\Delta f_1(x_1(t-\tau_1))M + \sum_{i=1}^{2} S_1^2(t)\,q_{i1}^2(S_1(t))\\ &-\sum_{i=1}^{2} S_1^2(t-\tau_i)\,q_{i1}^2(S_1 t-\tau_i) + \frac{1}{\gamma_1}\tilde{\theta}_1^T\dot{\widehat{\theta}}_1 + \frac{1}{\Gamma_1}\tilde{\sigma}\dot{\widehat{\sigma}},\end{aligned} \tag{16}$$

where $\tan(\cdot)$ and $\sec(\cdot)$ stand for tangent function and secant function, respectively. $M = \tan(\frac{\pi}{2\beta}S_1(t)) + \frac{\pi}{2\beta}S_1(t)\sec^2(\frac{\pi}{2\beta}S_1(t))$.

According to the Assumption1 and Young's inequality, there exist

$$\begin{cases}\Delta f_1(x_1(t-\tau_1))M \le \frac{1}{4}M^2 + S_1^2(t-\tau_1)\\ \quad q_{11}^2(S_1(t-\tau_1))\\ My_2 \le \frac{1}{2}M^2 + \frac{1}{2}y_2^2\end{cases}. \tag{17}$$

Therefore,

$$\begin{aligned}\dot{V}_1 \le{}& \left[\sigma S_2 + \sigma\alpha_2 + \tfrac{1}{2}\sigma M + \tfrac{1}{4}M + \theta_1^T\xi_1 - \tau_1\dot{y}_r\right]\\ &M + \tfrac{1}{2}\sigma y_2^2 + D_1 + \sum_{i=1}^{2} S_1^2(t)q_{i1}^2(S_1(t))\\ &+\tfrac{1}{\gamma_1}\tilde{\theta}_1^T\dot{\widehat{\theta}}_1 + \tfrac{1}{\Gamma_1}\tilde{\sigma}\dot{\widehat{\sigma}},\end{aligned} \tag{18}$$

where $D_1 = S_1^2(t-\tau_1)\,q_{11}^2(S_1(t-\tau_1)) - \sum_{i=1}^{2} S_1^2(t-\tau_i)\,q_{i1}^2(S_1(t-\tau_i))$.

The virtual control and adaptive laws are designed as below:

$$\alpha_2 = \frac{\widehat{\sigma}}{\widehat{\sigma}^2 + \eta_1}\begin{pmatrix}\left(-k_1 - \frac{1}{4} - \frac{1}{2}\widehat{\sigma}\right)M - \widehat{\theta}_1^T\xi_1 +\\ \tau_1\dot{y}_r - \frac{2\beta}{\pi}\sum_{i=1}^{2} S_1(t)\,q_{i1}^2(S_1(t))\end{pmatrix} \tag{19}$$

$$\dot{\widehat{\theta}}_1 = \gamma_1\left(\xi_1 M - m_1\widehat{\theta}_1\right) \tag{20}$$

$$\dot{\widehat{\sigma}} = \Gamma_1\left(M\alpha_2 - c_1\widehat{\sigma}\right), \tag{21}$$

where k_1, m_1, γ_1, c_1, and a_1 are the design constants, and η_1 is a small positive constant.

Remark 1 The estimation errors are given as $\tilde{\theta}_1 = \widehat{\theta}_1 - \theta_1$ and $\tilde{\sigma} = \widehat{\sigma} - \sigma$, and $\hat{\theta}_1$, $\widehat{\sigma}$ are the estimation of vector θ_1, $\widehat{\sigma}$, respectively.

From the Eq. (19–21), it obtains that

$$\begin{aligned}\dot{V}_1 \le{}& \left\{\begin{array}{l}\sigma S_2 - \tilde{\sigma}\alpha_2 - \frac{\eta_1}{\widehat{\sigma}^2+\eta_1}\left[\begin{array}{l}\left(-k_1 - \frac{1}{4} - \frac{1}{2}\widehat{\sigma}\right)M - \widehat{\theta}_1^T\xi_1\\ +\tau_1\dot{y}_r - \frac{2\beta}{\pi}\sum_{i=1}^{2} S_1(t)q_{i1}^2(S_1(t))\end{array}\right]\\ -\left(k_1 M + \frac{2\beta}{\pi}\sum_{i=1}^{2} S_1(t)q_{i1}^2(S_1(t)) + \frac{1}{2}\tilde{\sigma}M + \tilde{\theta}_1^T\xi_1\right)\end{array}\right\}\\ &M + \frac{1}{2}\sigma y_2^2 + D_1 + \sum_{i=1}^{2} S_1^2(t)q_{i1}^2(S_1(t)) + \tilde{\theta}_1^T\xi_1 M + \tilde{\sigma}M\alpha_2\\ &-m_1\tilde{\theta}_1^T\widehat{\theta}_1 - c_1\tilde{\sigma}\widehat{\sigma}\\ &\le \sigma M S_2 - k_1 M^2 - \frac{1}{2}\tilde{\sigma}M^2 + \frac{1}{2}\sigma y_2^2 + D_1 - c_1\tilde{\sigma}\widehat{\sigma}\\ &+\sum_{i=1}^{2}\left[S_1^2(t) - \frac{2\beta}{\pi}S_1(t)M\right]q_{i1}^2(S_1(t)) - m_1\tilde{\theta}_1^T\widehat{\theta}_1\\ &\le \sigma M S_2 - k_1 M^2 - \frac{1}{2}\tilde{\sigma}M^2 + \frac{1}{2}\sigma y_2^2\\ &+D_1 - \frac{1}{2}m_1\tilde{\theta}_1^2 - \frac{1}{2}c_1\tilde{\sigma}^2 + \frac{1}{2}m_1\theta_1^2 + \frac{1}{2}c_1\sigma^2.\end{aligned} \tag{22}$$

Remark 2 $-m_1\tilde{\theta}_1\widehat{\theta}_1 \le -\frac{1}{2}m_1\tilde{\theta}_1^2 + \frac{1}{2}m_1\theta_1^2$, $-c_1\tilde{\sigma}\widehat{\sigma} \le -\frac{1}{2}c_1\tilde{\sigma}^2 + \frac{1}{2}c_1\sigma^2$, $S_1^2(t) - \frac{2\beta}{\pi}S_1(t)M \le S_1^2(t)\left(1 - \sec^2\left(\frac{\pi}{2\beta}S_1(t)\right)\right) \le 0$.

Step 2: Filter α_2 through the following first-order filter with a time constant τ_2:

$$\tau_2\dot{\alpha}_{2f} + \alpha_{2f} = \alpha_2, \alpha_{2f}(0) = \alpha_2(0). \tag{23}$$

Then, one has

$$\dot{\alpha}_{2f} = -\frac{y_2}{\tau_2}. \tag{24}$$

Define the filter error of the first-order subsystem: $y_2 = \alpha_{2f} - \alpha_2$. Take the time derivative of y_2, and obtain

$$\left|\dot{y}_2 + \frac{y_2}{\tau_2}\right| \leq B_2\left(M, S_1, S_2, y_2, \widehat{\theta}, \widehat{\sigma}, q_{11}, q_{21}, y_r, \dot{y}_r, \ddot{y}_r\right). \tag{25}$$

Consequently, a calculation produces the following inequality:

$$y_2\dot{y}_2 \leq -\frac{y_2^2}{\tau_2} + y_2^2 + \frac{1}{4}B_2^2, \tag{26}$$

where B_2 is the continuous function.

Then, the derivative of S_2 is presented as below:

$$\dot{S}_2 = \frac{1}{\tau_2}\left[f_2 + u_q + \Delta f_2\left(\bar{x}_2\left(t-\tau_2\right)\right)\right] - \dot{\alpha}_{2f}, \tag{27}$$

where $f_2 = -x_2 - x_1 - x_1x_3$.

To facilitate its application in engineering, the RBFNN is used to approximate the nonlinear function f_2 again. So there exists a RBFNN system such that

$$f_2 = \theta_2^T\xi_2 + \varepsilon_2, \tag{28}$$

where ε_2 is the approximation error and satisfies $|\varepsilon_2| \leq \varepsilon_M$.

Substituting Eq. (28) into Eq. (27), it yields

$$\dot{S}_2 = \frac{1}{\tau_2}\left[\theta_2^T\xi_2 + u_q + \Delta f_2(\bar{x}_2(t-\tau_2))\right] - \dot{\alpha}_{2f}. \tag{29}$$

Choose the Lyapunov function candidate as below:

$$\begin{aligned} V_2 &= V_1 + \tfrac{1}{2}\tau_2 S_2^2 + \tfrac{1}{2}y_2^2 + \tfrac{1}{2\gamma_2}\tilde{\theta}_2^T\tilde{\theta}_2 \\ &+ \int_{t-\tau_2}^{t} S_2^2(\tau)q_{22}^2(\bar{S}_2(\tau))d\tau. \end{aligned} \tag{30}$$

The time derivative of V_2 is given as below:

$$\begin{aligned} \dot{V}_2 \leq\ & \dot{V}_1 + S_2\left(\theta_2^T\xi_2 + u_q - \tau_2\dot{\alpha}_{2f}\right) \\ & + S_2\Delta f_2\left(\bar{x}_2\left(t-\tau_2\right)\right) + \left(1 - \frac{1}{\tau_2}\right)y_2^2 + \frac{1}{4}B_2^2 \\ & + \frac{1}{\gamma_2}\tilde{\theta}_2^T\dot{\widehat{\theta}}_2 + S_2^2\left(t\right)q_{22}^2\left(\bar{S}_2\left(t\right)\right) \\ & - S_2^2\left(t-\tau_2\right)q_{22}^2\left(\bar{S}_2\left(t-\tau_2\right)\right). \end{aligned} \tag{31}$$

Note the following inequality:

$$\begin{aligned} S_2\Delta f_2(\bar{x}_2(t-\tau_2)) \leq\ & \frac{1}{4}S_2^2 + S_1^2(t-\tau_2)q_{21}^2(S_1(t-\tau_2)) \\ & + S_2^2(t-\tau_2)q_{22}^2(\bar{S}_2(t-\tau_2)). \end{aligned} \tag{32}$$

Substituting Eq. (32) into Eq. (31), the equation can be rewritten as

$$\begin{aligned} \dot{V}_2 \leq\ & -k_1M^2 - \frac{1}{2}\tilde{\sigma}M^2 + \frac{1}{2}\sigma y_2^2 + D_1 - \frac{1}{2}m_1\tilde{\theta}_1^2 \\ & -\frac{1}{2}c_1\tilde{\sigma}^2 + \frac{1}{2}m_1\theta_1^2 + \frac{1}{2}c_1\sigma^2 + S_2\left[\theta_2^T\xi_2 + \right. \\ & \left.\sigma M + u_q - \tau_2\dot{\alpha}_{2f} + \frac{1}{4}S_2 + S_2(t)q_{22}^2(\bar{S}_2(t))\right] \\ & + D_2 + \left(1 - \frac{1}{\tau_2}\right)y_2^2 + \frac{1}{4}B_2^2 + \frac{1}{\gamma_2}\tilde{\theta}_2^T\dot{\widehat{\theta}}_2, \end{aligned} \tag{33}$$

where $D_2 = S_1^2(t-\tau_2)q_{21}^2(S_1(t-\tau_2))$.

In the same way, the control law and adaptive law are given as the following forms:

$$\begin{aligned} u_q =\ & -k_2S_2 - \sigma M - \widehat{\theta}_2^T\xi_2 + \tau_2\dot{\alpha}_{2f} - \frac{1}{4}S_2 \\ & -S_2(t)q_{22}^2(\bar{S}_2(t)) \end{aligned} \tag{34}$$

$$\dot{\widehat{\theta}}_2 = \gamma_2\left(\xi_2S_2 - m_2\widehat{\theta}_2\right), \tag{35}$$

where k_2, m_2 and γ_2 are the design constant.

With Eq. (34) and Eq. (35), Eq. (33) is written as follows:

$$\begin{aligned} \dot{V}_2 \leq\ & -\left(k_1 + \frac{1}{2}\tilde{\sigma}\right)M^2 + \left(1 + \frac{1}{2}\sigma - \frac{1}{\tau_2}\right) \\ & -S_2\widehat{\sigma}My_2^2 - k_2S_2^2 + \sum_{i=1}^{2}D_i + \frac{1}{4}B_2^2 - \frac{1}{2}c_1\tilde{\sigma}^2 \\ & -\frac{1}{2}\sum_{i=1}^{2}m_i\tilde{\theta}_i^2 + \frac{1}{2}c_1\sigma^2 + \frac{1}{2}\sum_{i=1}^{2}m_i\theta_i^2. \end{aligned} \tag{36}$$

Remark 3 The estimation error is written as $\tilde{\theta}_2 = \widehat{\theta}_2 - \theta_2$, and $\hat{\theta}_2$ is the estimation of vector θ_2, $-m_2\tilde{\theta}_2\ \widehat{\theta}_2 \leq -\frac{1}{2}m_2\tilde{\theta}_2^2 + \frac{1}{2}m_2\theta_2^2$.

Step 3: The time derivative of S_3 is obtained as

$$\begin{aligned} \dot{S}_3 &= \frac{1}{\tau_1}\left[x_1x_2 - x_3 + u_d + \Delta f_3(x_3(t-\tau_3))\right] \\ &= \frac{1}{\tau_1}\left[f_3 + u_d + \Delta f_3(x_3(t-\tau_3))\right], \end{aligned} \tag{37}$$

where $f_3 = x_1x_2 - x_3$.

Similarly, for simplicity, there exists a RBFNN system such that

$$f_3 = \theta_3^T\xi_3 + \varepsilon_3, \tag{38}$$

where ε_3 is the approximation error and satisfies

$|\varepsilon_3| \leq \varepsilon_M$.

Choose the Lyapunov function candidate as

$$V_3 = V_2 + \frac{1}{2}\tau_3 S_3^2 + \frac{1}{2\gamma_3}\tilde{\theta}_3^T\tilde{\theta}_3 + \int_{t-\tau_3}^{t} S_3^2(\tau)q_{31}^2(S_3(\tau))d\tau. \tag{39}$$

Then, the derivative of V_3 is calculated as below:

$$\dot{V}_3 = \dot{V}_2 + S_3\left(\theta_3^T\xi_3 + u_\mathrm{d}\right) + S_3\Delta f_3\left(x_3(t-\tau_3)\right) + \frac{1}{\gamma_3}\tilde{\theta}_3^T \dot{\widehat{\theta}}_3 + S_3^2(t)q_{31}^2\left(S_3(t)\right) + S_3^2(t-\tau_3)q_{31}^2\left(S_3(t-\tau_3)\right). \tag{40}$$

According to Eq. (6), the following inequality yields:

$$S_3\Delta f_3(x_3(t-\tau_3)) \le \frac{1}{4}S_3^2 + S_3^2(t-\tau_3)q_{31}^2(S_3(t-\tau_3)). \tag{41}$$

Substituting Eq. (41) into Eq. (40), the equation can be rewritten as

$$\dot{V}_3 = -\left(k_1 + \frac{1}{2}\tilde{\sigma}\right)M^2 + \left(1 + \frac{1}{2}\sigma - \frac{1}{\tau_2}\right)y_2^2 - k_2S_2^2 + \sum_{i=1}^{2} D_i + \frac{1}{4}B_2^2 - \frac{1}{2}\sum_{i=1}^{2} m_i\tilde{\theta}_i^2 + S_3\left(\theta_3^T\xi_3 + u_\mathrm{d} + S_3(t)q_{31}^2(S_3(t)) + \frac{1}{4}S_3\right)$$

$$-\frac{1}{2}c_1\tilde{\sigma}^2 + \frac{1}{2}c_1\sigma^2 + \frac{1}{2}\sum_{i=1}^{2} m_i\theta_i^2 + \frac{1}{\gamma_3}\tilde{\theta}_3^T\dot{\widehat{\theta}}_3. \tag{42}$$

At the current stage, the control input is chosen as

$$u_\mathrm{d} = -k_3S_3 - \widehat{\theta}_3^T\xi_3 - \frac{1}{4}S_3 - S_3(t)q_{31}^2(S_3(t)), \tag{43}$$

where k_3 is the positive constant.

In addition, the update law is chosen as follows:

$$\dot{\widehat{\theta}}_3 = \gamma_3\left(\xi_3S_3 - m_3\widehat{\theta}\right), \tag{44}$$

where m_3 and γ_3 are the design constant.

Substituting Eq. (43–44) into Eq. (42), the time derivative of V_3 is rewritten as follows:

$$\dot{V}_3 = -\left(k_1 + \frac{1}{2}\tilde{\sigma}\right)M^2 + \left(1 + \frac{1}{2}\sigma - \frac{1}{\tau_2}\right)y_2^2 - k_2S_2^2 - k_3S_3^2 + \sum_{i=1}^{2} D_i - \frac{1}{2}\sum_{i=1}^{3} m_i\tilde{\theta}_i^2 + \frac{1}{4}B_2^2 - \frac{1}{2}c_1\tilde{\sigma}^2 + \frac{1}{2}c_1\sigma^2 + \frac{1}{2}\sum_{i=1}^{3} m_i\theta_i^2. \tag{45}$$

Remark 4 The estimation error is expressed as $\tilde{\theta}_3 = \widehat{\theta}_3 - \theta_3$, and $\hat{\theta}_3$ is the estimation of vector θ_3, $-m_3\tilde{\theta}_3\widehat{\theta}_3 \le -\frac{1}{2}m_3\tilde{\theta}_3^2 + \frac{1}{2}m_3\theta_3^2$.

Up to now, the whole design process of the controller of BLDCM is completed. The schematic plan of proposed control method is depicted in Fig. 6.

4 Stability analysis

For any given $p > 0$, the closed sets can be defined as follows:

$$\begin{cases} \Pi_1 = \left\{ \begin{array}{l} (M, S_1, \widehat{\theta}_1, \widehat{\sigma}, q_{11}, q_{12}) : M^2 + \frac{1}{\gamma_1}\tilde{\theta}_1^2 + \frac{1}{\Gamma_1}\tilde{\sigma}^2 \\ +2\sum_{i=1}^{2}\int_{t-\tau_i}^{t} S_1^2(\tau)q_{i1}^2(S_1(\tau))d\tau \le 2p \end{array} \right\} \\ \Pi_2 = \left\{ \begin{array}{l} (M, S_1, S_2, \widehat{\theta}_1, \widehat{\theta}_2, \widehat{\sigma}, y_2, q_{11}, q_{12}, q_{22}) : M^2 + S_2^2 + y_2^2 \\ +\sum_{i=1}^{2}\frac{1}{\gamma_i}\tilde{\theta}_i^2 + \frac{1}{\Gamma_1}\tilde{\sigma}^2 + 2\int_{t-\tau_2}^{t} S_2^2(\tau)q_{22}^2(\bar{S}_2(\tau))d\tau \le 2p \end{array} \right\} \\ \Pi_3 = \left\{ \begin{array}{l} (M, S_1, S_2, S_3, \widehat{\theta}_1, \cdots, \widehat{\theta}_3, \widehat{\sigma}, y_2, q_{11}, q_{12}, q_{22}, q_{31}) : M^2 \\ +\sum_{i=2}^{3} S_i^2 + y_2^2 + \sum_{i=1}^{3}\frac{1}{\gamma_i}\tilde{\theta}_i^2 + \frac{1}{\Gamma_1}\tilde{\sigma}^2 + 2\int_{t-\tau_3}^{t} S_3^2(\tau)q_{31}^2(S_3(\tau))d\tau \le 2p \end{array} \right\} \end{cases}. \tag{46}$$

Theorem 2 *Suppose that the dynamic surface controllers Eq. (34) and (43) with adaptive laws Eq. (20),(21) (35), and (44) are applied to the BLDCM system with the uncertain time delays described by Eq. (4), by selecting the proper parameters like k_i, γ_i, m_i, Γ_1, η_1, τ_2, and c_1, then the $S_1(t)$ is asymptotically tracking stability in the sense of uniformly ultimate boundedness when the initial conditions satisfy the Π_i and*

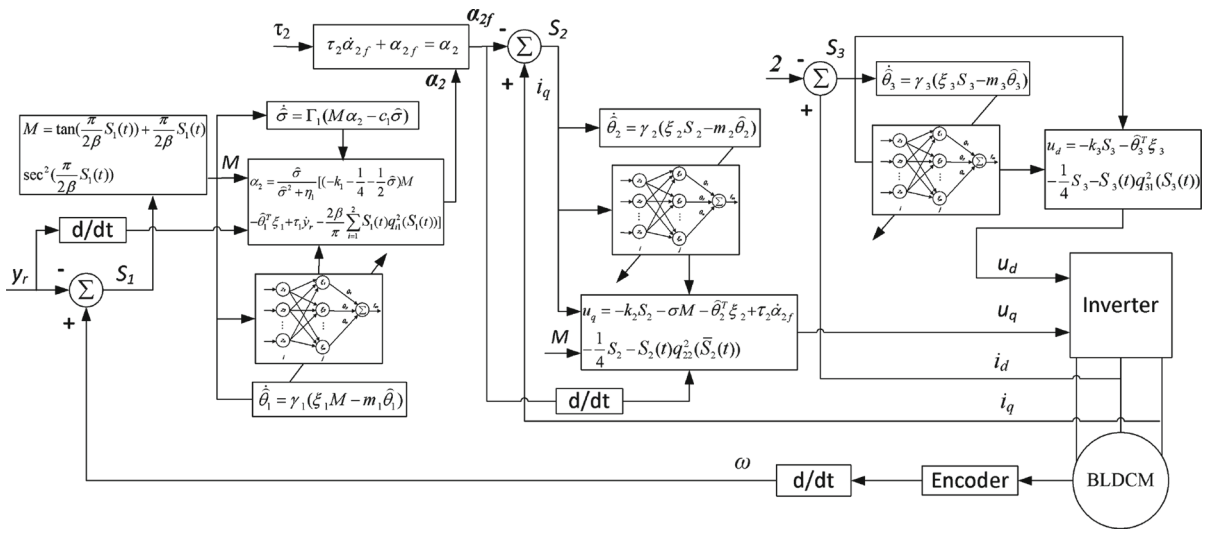

Fig. 6 Control schematic of BLDCM

$x_1(0) \in (-a + d + y_r(0),\ a - d + y_r(0))$. *Furthermore, the state* $x_1(t)$ *can keep in the set* $\Omega := \{x_1(t) \in R : |x_1(t)| < a\}$ *and error state* $S_1(t) \in (-\beta,\ \beta)$ *for* $\forall t > 0$.

Proof First, calculate the derivative of the Lyapunov function candidate as

$$\dot{V} = \dot{V}_3 = -\left(k_1 + \tfrac{1}{2}\tilde{\sigma}\right) M^2 - k_2 S_2^2 - k_3 S_3^2 + \left(1 + \tfrac{1}{2}\sigma - \tfrac{1}{\tau_2}\right) y_2^2 - \tfrac{1}{2}\sum_{i=1}^{3} m_i \tilde{\theta}_i^2 - \tfrac{1}{2} c_1 \tilde{\sigma}^2 + \sum_{i=1}^{2} D_i + \tfrac{1}{4} B_2^2 + \tfrac{1}{2} c_1 \sigma^2 + \tfrac{1}{2}\sum_{i=1}^{3} m_i \theta_i^2. \quad (47)$$

If $V = p$, taking those pre-mentioned into account, then there exists

$$\dot{V} \le -2a_0 V + \mu, \quad (48)$$

where $\mu = \sum_{i=1}^{2} D_i + \frac{1}{4} B_2^2 + \frac{1}{2} c_1 \sigma^2 + \frac{1}{2}\sum_{i=1}^{3} m_i \theta_i^2$.

If $V = p$ and $a_0 > \mu/p$, then $\dot{V} \le 0$. As the initial condition $V(0) \le p$, one has $V(t) \le p,\ \forall t \ge 0$.

Let Eq.(48) be compute the integral on $[0\ t]$, then

$$0 \le V(t) \le \frac{\mu}{a_0} + (V(0) - \frac{\mu}{a_0}) e^{-2a_0 t}. \quad (49)$$

Second, note the fact that $S_1(t)\tan((\pi/2\beta) \times S_1(t)) \to \infty$ as $S_1(t) \to \beta$ or - β. Since $S_1(t)$ and $S_1(t)\tan((\pi/2\beta) \times S_1(t))$ is uniformly ultimately bounded, there exists $S_1(t) \ne -\beta$ and $S_1(t) \ne \beta$. Let give initial condition $S_1(t) \in (-\beta,\ \beta)$, it can be concluded that $S_1(t)$ remains in the region $(-\beta,\ \beta)$ for $\forall t > 0$. Furthermore, owing to the fact $\beta = a - d$, the following relations hold:

$$-a + d < S_1(t) < a - d \Leftrightarrow -a + d + y_r < x_1(t) < a - d + y_r. \quad (50)$$

Then, with the fact $d + y_r \ge 0$ and $-d + y_r \le 0$, it is obtained that $-a < x_1(t) < a$. Up to now, the proof is completed.

5 Performance evaluation

In this section, the numerical simulations are conducted in order to validate the feasibility and effectiveness of the proposed method. Meanwhile, it is mainly utilized to verify the performance of the BLDCM with chaotic behavior and parameter variation.

Taking into account uncertain time delay, the relative equations can be described by

$$\Delta f_1(x_1(t - \tau_1)) = \sin(x_1(t - \tau_1)),$$
$$\Delta f_2(\bar{x}_2(t - \tau_2)) = x_1(t - \tau_2) x_2(t - \tau_2),$$
$$\Delta f_3(x(t - \tau_3)) = \sin(x_3(t - \tau_3)). \quad (51)$$

The part of system parameters are given as $q_{11} = 1, q_{21} = 1 - \sqrt{2 - S_1^2}$, $q_{22} = |S_2|, q_{31} = 0$, $\tau_1 = 0.4$, $\tau_2 = 0.5$, $\tau_3 = 0.6$, and the rest are the same as ones mentioned before.

Suppose that the state is required to constraint $|x_1(t)| < 1.2$, and the reference signal is $-1.0 \le y_r = 0.7^*\sin(4t) + 0.2^*\cos(2t + 0.3) \le 1.0$; meanwhile, the corresponding design parameter is chosen as $\beta = |x_1| - |y_r| = 0.2$. The simulations are done with initial conditions $x_1(0) = 0 \in (-0.2, 0.2)$, $x_2(0) = 0.45$, $x_3(0) = 0.4$. The design parameters of controller

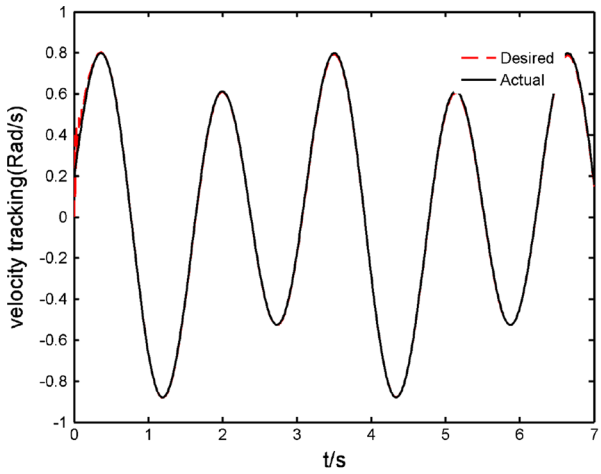

(a) The rotor velocity tracking.

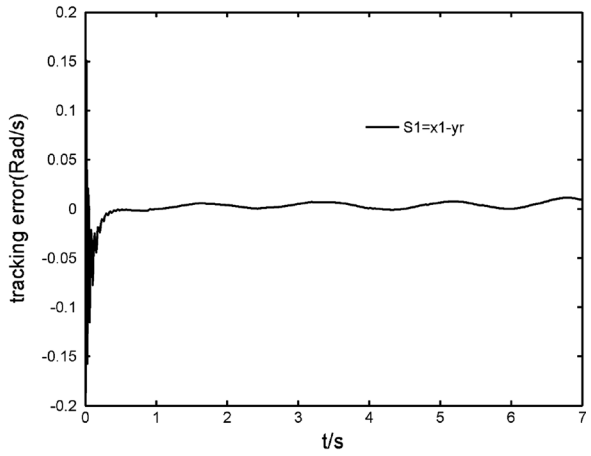

(b) The rotor velocity tracking error.

Fig. 7 The trajectory tracking with parameter $\eta = 1.6$. **a** The rotor velocity tracking, **b** the rotor velocity tracking error

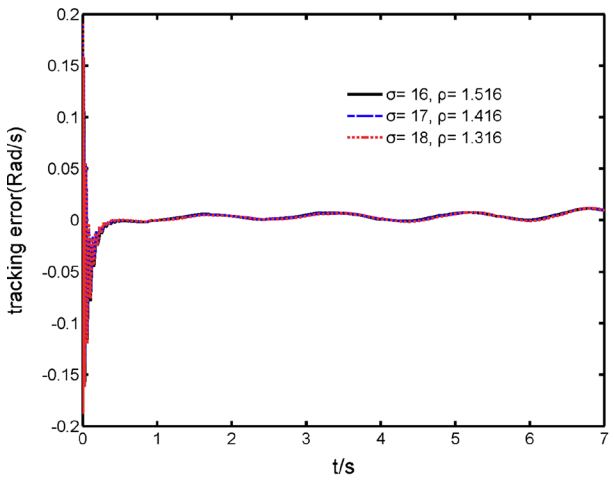

(a) The rotor velocity tracking error.

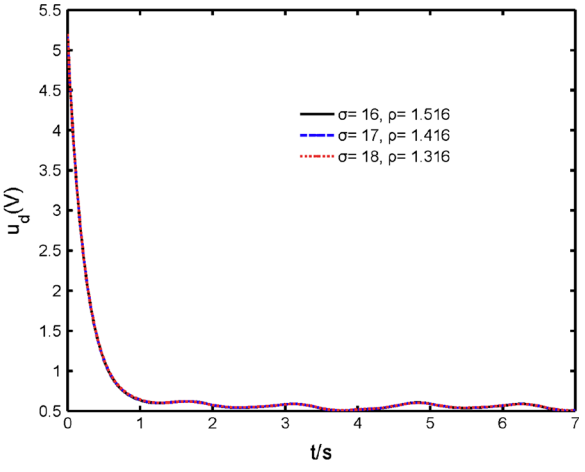

(b) d axis voltage.

Fig. 8 The robustness analysis with parameter variation. **a** The rotor velocity tracking error, **b** *d* axis voltage

are chosen as $k_1 = k_2 = 1$, $k_3 = 3$, $\gamma_1 = \gamma_2 = \gamma_3 = 12$, $m_1 = m_2 = m_3 = 0.5$, $c_1 = 0.8$, $r_1 = 0.2$, $\sigma(0) = 35$, $\eta_1 = 0.001$, $\tau_2 = 0.01$. In addition, the center of neural network μ_i is uniformly distributed in the field of [−5,5], and its width σ_i is equal to 2.

5.1 Trajectory tracking analysis

Figure 7 shows that the steady-state error of velocity is equal to ±0.01 Rad/s with little time. On the other hand, it can be seen clearly that the system tracks the desired trajectory perfectly within 0.1s. The state $|x_1(t)| < 1.2$ is ensured by the fact that tracking error $S_1(t) \in (-0.2, 0.2)$ when the TBLF is used.

5.2 Robustness analysis

Figure 8 shows the results of the BLDCM control performance when disturbance of the system parameters σ and ρ occurs, i.e., $\sigma = 16$, $\rho = 1.516$, $\sigma = 17$, $\rho = 1.416$, $\sigma = 18$, $\rho = 1.316$. When the system parameters add or reduce the value a bit, the three kinds

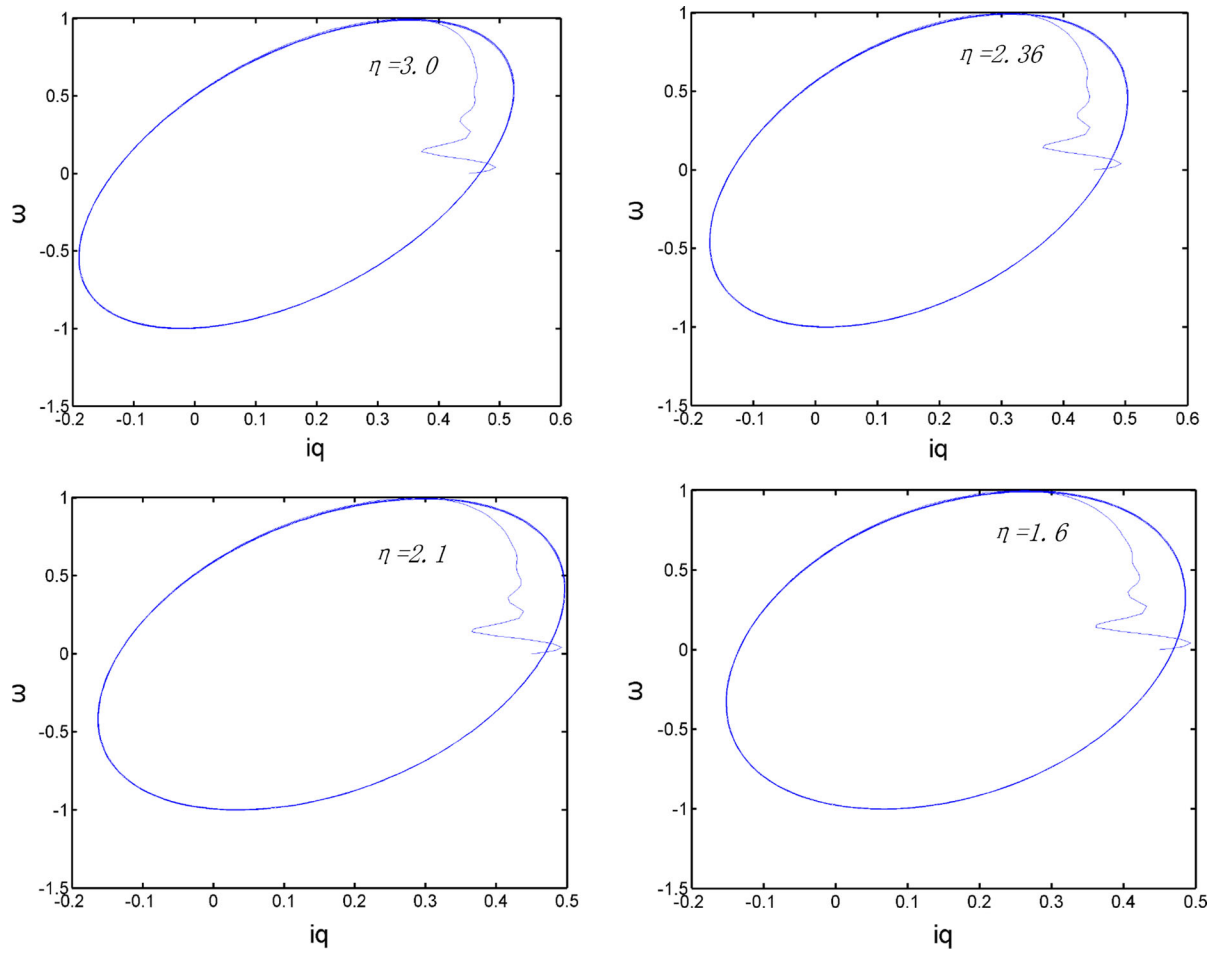

Fig. 9 Phase portrait with different η

of indicator curves of BLDCM can basically coincide. That is, the proposed controller owns good robustness for disturbance in whole process.

5.3 Chaos suppression analysis

Comparing with the result mentioned above, it can be seen clearly that BLDCM system successfully escapes from the chaotic behavior which can cause some irreparable losses on the local power system in the Fig. 9.

6 Conclusion

An adaptive RBFNN-based DSC strategy is presented for the chaotic BLDCM with uncertain time delays in detail. The controller based on the adaptive DSC, TBLF, and RBFNN is applied to prevent the motor drive system from chaos when systemic parameters are falling into a special area. Both the unknown BLDCM parameters and uncertain time delays are considered. At the same time, the state constraint is satisfied using TBLF. In addition, the stability analysis is derived to verify the system reliability by the Lyapunov theory. Finally, the simulation results are demonstrated to show the effectiveness and robustness of the proposed approach by choosing appropriate design parameters.

Acknowledgments This work is supported by the National Natural Science Foundation of China (Grant Nos. 51375506), the Specialized Research Fund for the Doctoral Program of Higher Education (Grant No. 20100191110008), China Postdoctoral Science Foundation funded project (Grant No. 2013M542258) and the Par-Eu Scholars Program Special Foundation of Chongqing.

References

1. Ditto, W.L., Spano, M.L., Savage, H.T., Rauseo, S.N., Heagy, J., Ott, E.: Experimental observation of a strange nonchaotic attractor. Phys. Rev. Lett. **65**, 533–536 (1990)
2. Wang, Z., Chau, K.T.: Anti-control of chaos of a permanent magnet DC motor system for vibratory compactors. Chaos Solitons Fractals **36**, 694–708 (2008)
3. Li, D., Wang, S.L., Zhang, X.H., Yang, D.: Fuzzy impulsive control of chaos in permanent magnet synchronous motors with parameter uncertainties. Acta Phys. Sin. **58**, 1432–1440 (2009)
4. Hernandez-Guzman, V.M., Santibanez, V., Zavala-Rio, A.: A saturated PD controller for robots equipped with brushless DC-motors. Robotica **28**, 405–411 (2010)
5. Huang, X.Y., Goodman, A., Gerada, C., Fang, Y.T., Lu, Q.F.: Design of a five-phase brushless DC motor for a safety critical aerospace application. IEEE Trans. Ind. Electron. **59**, 3532–3541 (2012)
6. Feng, Y., Yu, X.H., Man, Z.H.: Non-singular terminal sliding mode control of rigid manipulators. Automatica **38**, 2159–2167 (2002)
7. Estrada, A., Fridman, L.: Quasi-continuous HOSM control for systems with unmatched perturbations. Automatica **46**, 1916–1919 (2010)
8. Alasty, A., Salarieh, H.: Controlling the chaos using fuzzy estimation of OGY and Pyragas controllers. Chaos Solitons Fractals **26**, 379–392 (2005)
9. Paula, A.S.D., Savi, M.A.: A multi-parameter chaos control method based on OGY approach. Chaos Solitons Fractals **40**, 1376–1390 (2009)
10. Zhang, C.M., Liu, H.P., Chen, S.J., Wang, F.J.: Application of neural network for permanent magnet synchronous motor direct torque control. J. Syst. Eng. Electron. **19**, 555–561 (2008)
11. Elmas, C., Ustun, O., Sayan, H.H.: A neuro-fuzzy controller for speed control of a permanent magnet synchronous motor drive. Expert Syst. Appl. **34**, 657–664 (2008)
12. Ge, Z.M., Cheng, J.W., Chen, Y.S.: Chaos anticontrol and synchronization of three time scales brushless DC motor system. Chaos Solitons Fractals **22**, 1165–1182 (2004)
13. Ge, Z.M., Chang, C.M., Chen, Y.S.: Anti-control of chaos of single time scale brushless dc motors and chaos synchronization of different order systems. Chaos Solitons Fractals **27**, 1298–1315 (2006)
14. Ngo, K.B., Mahony, R., Jiang, Z.P.: Integrator backstepping using barrier functions for systems with multiple state constraints. In: Proc 44th IEEE Conf. on Decision and Control, and the European Control Conf., 8306–8312 (2005)
15. Tee, K.P., Ge, S.S., Tay, E.H.: Barrier Lyapunov functions for the control of output-constrained nonlinear systems. Automatica **45**, 918–927 (2009)
16. Luo, X., Wu, X., Guan, X.: Adaptive backstepping control for unmatched nonlinear system against actuator dead-zone fault. IET Control Theory Appl. **4**, 879–888 (2010)
17. Wu, X.L., Wu, X.J., Luo, X.Y., Zhu, Q.M., Guan, X.P.: Neural network-based adaptive tracking control for nonlinearly parameterized systems with unknown input nonlinearities. Neurocomputing **82**, 127–142 (2012)
18. Wei, D.Q., Luo, X.S., Wang, B.H., Fang, J.Q.: Robust adaptive dynamic surface control of chaos in permanent magnet synchronous motor. Phys. Lett. A **363**, 71–77 (2007)
19. Zhang, X.Y., Lin, Y.: A robust adaptive dynamic surface control for nonlinear systems with hysteresis input. Acta Autom. Sin. **36**, 1264–1271 (2010)
20. Ma, H., Deshmukh, V., Butcher, E., Averina, V.: Delayed state feedback and chaos control for time-periodic systems via a symbolic approach. Commun. Nonlinear Sci. Numer. Simul. **10**, 479–497 (2005)
21. Wu, X.J., Wu, X.L., Luo, X.Y., Guan, X.P.: Dynamic surface control for a class of state-constrained non-linear systems with uncertain time delays. IET Control Theory Appl. **6**, 1948–1957 (2012)
22. Li, Y.M., Ren, C.E., Tong, S.C.: Adaptive fuzzy backstepping output feedback control for a class of MIMO time-delay nonlinear systems based on high-gain observer. Nonlinear Dyn. **67**, 1175–1191 (2012)
23. Li, Y., Tong, S.C., Li, Y.M.: Observer-based adaptive fuzzy backstepping dynamic surface control design and stability analysis for MIMO stochastic nonlinear systems. Nonlinear Dyn. **69**, 1333–1349 (2012)
24. Ge, Z.M., Cheng, J.W.: Chaos synchronization and parameter identification of three time scales brushless DC motor system. Chaos Solitons Fractals **24**, 597–616 (2005)
25. Michael Steele, J.: The Cauchy–Schwarz Master Class: An Introduction to the Art of Mathematical Inequalities, Chapter 1. Cambridge University Press, Cambridge (2004)